Applied Catalysis B: Environmental 231 (2018) 391–399

Contents lists available at ScienceDirect

Applied Catalysis B: Environmental

journal homepage: www.elsevier.com/locate/apcatb

NO_x adsorption on K and Ba loaded on zirconia-titania NSR catalysts: A comparative study by *in situ* and *operando* IR spectroscopy

Hai P. Nguyen[a,*], Sandra Palma Del Valle[b], Olivier Marie[b]

[a] Toyota Motor Europe, 1930 Zaventem, Belgium
[b] LCS UMR6506 UNICAEN – ENSICAEN, France

ARTICLE INFO

Keywords:
NSR
NO_x adsorption
Cation chemical hardness
Potassium
Zirconia-titania
Barium

ABSTRACT

An intensive *in situ* and *operando* IR study on NO_x adsorption over potassium (K) loaded zirconia-titania NSR catalyst in comparison to a barium (Ba) loaded one is reported. Based on *in situ* IR experiments, NO_x adsorption under heated environment was confirmed to favor potassium bidentate nitrate species rather than ionic nitrate species observed for Ba-loaded NSR catalyst (previously published). Complementary *operando* IR experiments revealed different mechanisms for NO_x adsorption over the two NO_x storage materials (NSMs): initial simultaneous NO_2^- and NO_3^- formation over K loaded catalyst while over Ba-loaded one, NO_2^- is first accumulated before being converted to NO_3^-. Isotopic labelling in combination with *operando* experiments identified distinct dynamic behaviors regarding the exchange between nitrogen containing species on surface and in gas phase. This work provides beneficial inputs for advanced catalyst converter design, for example with zone-coated washcoat that contains more than one catalyst formulations.

1. Introduction

The NO_x storage and reduction (NSR) or lean NO_x trap (LNT) has been a vital solution for Diesel or gasoline lean-burn engines as it can efficiently catalyse NO_x to harmless nitrogen [1–4]. The original and typical NSR catalytic formulation consists of platinum (Pt) and barium (Ba) supported onto alumina ($\gamma - Al_2O_3$) [1,2]. Many studies have been performed providing insights into the mechanisms of involved catalytic reactions over this NSR formulation, as in selected literature [5–8]. Several comprehensive reviews can also be found [3,9]. NSR catalysts are known to have some critical issues such as the sulfur poisoning and thermal degradation, which have been tackled and reported. For example, Matsumoto and colleagues [10] pointed out that the sulfur poisoning was caused not only by interaction with the alkaline metal (Ba) to yield barium sulfates but also by interaction with the alumina support material. They therefore suggested to add an acidic material such as TiO_2 or ZrO_2 to the conventional $\gamma - Al_2O_3$ support material leading to materials able to minimize the SOx adsorption and thus to enhance barium sulphate desorption. Furthermore, the work by Imagawa and colleagues revealed that using nano-composites of Al_2O_3 and ZrO_2–TiO_2 (ZT) could both strongly enhance the thermal stability and lower the sulfur poisoning [8].

Similar conclusions were obtained by Kim et al., when studying the impact of ZrO_2 or TiO_2 on noble metal (Pt or Pd) loaded SiO_2 Diesel Oxidation catalysts. Indeed, the presence of both ZrO_2 or TiO_2 on SiO_2 lowers the amount of basic sites and thus limits sulphate formation while the noble metal dispersion is preserved due to a strong interaction between them and either ZrO_2 or TiO_2 giving the catalyst a higher hydrothermal stability.

One may however wonder about the resistance of the titania phase when submitted to high temperatures encountered during the DPF regeneration. Indeed, very little data are available in the literature regarding the hydrothermal stability of ZT mixed oxides, however Hirano et al. [11] reported that anatase-type TiO_2 doped with ZrO_2 shows high phase stability and maintains anatase-type structure even after heating at 1000 °C for 1 h. Furthermore, when incorporating Ti into the inorganic wall of ordered porous zirconium oxide via direct synthesis, Chen et al. [12] claimed that titanium ions are homogeneously dispersed into the framework of ZrO_2, when the amount of titanium doping is less than 20 mol% being a suitable loading to improve the thermal stability of porous zirconium oxide.

The NO_x adsorption step, as it plays an essential role to the overall performance of NSR catalysts, has been intensively studied and various NO_x storage materials (NSMs) such as alkaline metals potassium (K), strontium (Sr), lithium (Li), or calcium (Ca) were suggested as alternatives for barium. Potassium being the most promising candidate was thus widely studied [13–19]. One of the significant works were done by Toop et al. who provided great insights into mechanisms of NSR

* Corresponding author.
E-mail address: hai.p.nguyen@toyota-europe.com (H.P. Nguyen).

https://doi.org/10.1016/j.apcatb.2018.03.002
Received 12 December 2017; Received in revised form 23 February 2018; Accepted 1 March 2018
Available online 05 March 2018
0926-3373/

processes. At 350 °C and without Pt, they reported that NO_x are primarily adsorbed on alumina in the monodentate, chelating, and bridged forms. In another work, the same group showed that the NO_x adsorption increases with increasing K loadings [20]. They also provided evidence of two routes: one involving Pt sites and another NO_2 disproportionation route involving Pt-irrespective sites. It was also reported that nitrites species (NO_2^-) are only significant at low temperatures (below 200 °C) [21].

So far, works dealing with the direct comparison between Ba and K have already been described [22,23,18,24,25], however, all of these studies focused on alumina supported NSR formulations. It is noteworthy that support materials have been reported to greatly impact the NO_x ad/desorption during lean/rich cycling. For example, Piacentini et al. reported that NO_x storage not only takes place onto NSM but also onto the surface of support materials [26]. In our previous study [27], opposite behaviours were found for NO_x storage over Al_2O_3 or ZT: barium tends to form bigger particles during NO_x uptake process on alumina, while small (sub)nano-particles or thin layer of barium nitrates are favoured over ZT supported formulation. The present work thus focuses on the NO_x adsorption behaviour over a K loaded ZT NSR catalyst, which has never been reported with significant details. The comparison between K and Ba as NO_x storage materials supported on the same ZT support material is also investigated. In order to provide a clear picture of their distinct behaviour, the present work reports a model study using CO_2 and water free conditions. Competition between carbonates and nitrates formation will thus be avoided rendering possible a better identification of adsorbed NO_x species. Furthermore, the absence of water will be of great importance to clarify the intrinsic role of K and Ba, especially in the low temperature range were water assisted NO_2 disproportionation was reported to occur [28].

2. Materials/experiments

Two NSR formulations, Pt/ZT + K and Pt/ZT + Ba were supplied by Toyota. The Ba loading is 11 wt% while that for K is 2 wt%. Composition of the ZT solid solution is 70% ZrO_2 and 30% TiO_2. Both samples contain Pt 1 wt%. Specific surface areas of the catalysts are similar and about 100 $m^2\,g^{-1}$.

Aiming at studying the nature of absorbed entities, *in situ* IR spectroscopy was first applied (Fig. 1).Before the measurements, the samples were activated at 450 °C (for 1.5 h) under high vacuum ($p \approx 10^{-6}$ mbar). As carbonate traces remained on the surface after such a pre-treatment, three cycles of storage, reduction and evacuation were performed. One cycle consists in the introduction at 450 °C of an NO_2 equilibrium pressure (1.33 mbar) in contact with the sample during 10 min, the setup is then evacuated and 133 mbar of H_2 are further introduced for another 10 min before evacuation. The FTIR spectra of the activated samples were subtracted from those recorded after NO_2 adsorption. All the spectra reported in the present work are the results of this subtraction and are normalized to a similar weight of sample. It is noteworthy that in these *in situ* experiments, after the above described thermal pre-treatment, NO_2 was introduced on a pulse basis with a 5 min stabilizing period rather than under dynamic flow. This design allows to know surely the amount of NO_x adsorption on the catalyst and thus, to precisely quantify the NO_x uptake. The samples were then investigated in *operando* experiments in the transmittance mode, which allows the correlation between the evolution of adsorbed species and the gas phase one. Details of the design and methodology for both *in situ* and *operando* experiment can be found in our previous paper [27].

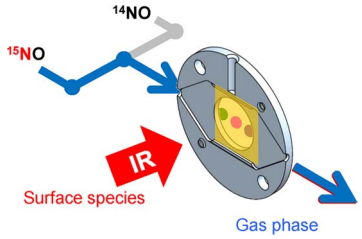

Fig. 2. Scheme of isotopic labelling operando experiments. Pure ^{14}NO or pure ^{15}NO was alternately mixed with O_2/Ar before feeding to the sample.

It should be noted that in the current work, an isotopic labelling methodology was applied during the *operando* experiments (Fig. 2). Isotopes of NO (^{14}NO or ^{15}NO) in a mixture consisting of 400 ppm NO, 1% O_2 balanced with Ar was alternatively introduced into the cell while surface species and gas phase were simultaneously monitored through FTIR and complementary FTIR & chemiluminiscence respectively. These experiments allowed to distinguish various nitrogen containing species on the surface and in the gas phase, and the dynamics of exchange between them.

3. Results and discussions

3.1. NO_x adsorption under in situ conditions

Although NO_x adsorption over K-loaded catalysts has been studied in the literature as discussed in section Introduction above, all the reported works were with alumina supported NSR formulations. The determination of the nature of adsorbed species (peak identification) on Pt/ZT + K was not found in literature. In the first series of experiments, the so-called 'regular' *in situ* experiments (Ex1 in Fig. 1), IR spectra were recorded after introduction of every NO_2 dose, with 5 min stabilizing time, at room temperature. NO_2 gas was selected for the *in situ*

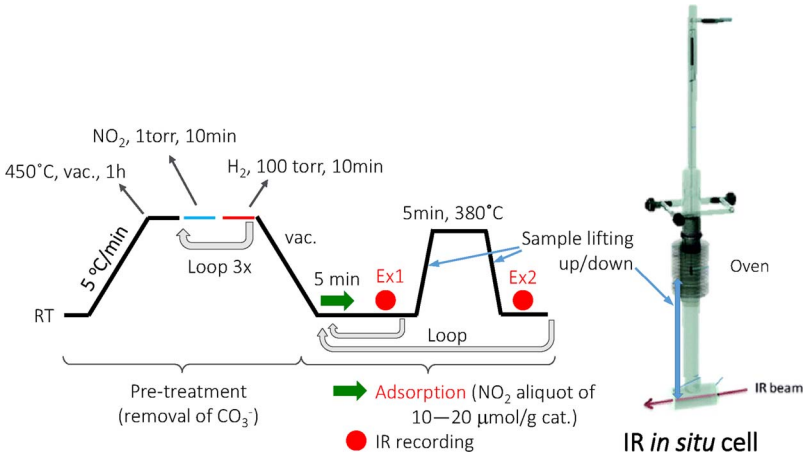

Fig. 1. Scheme for *in situ* experiments: (Ex1) IR spectra are recorded after each NO_2 dose; (Ex2) IR spectra are recorded after introducing NO_2 dose and heating at 380 °C for 5 min.

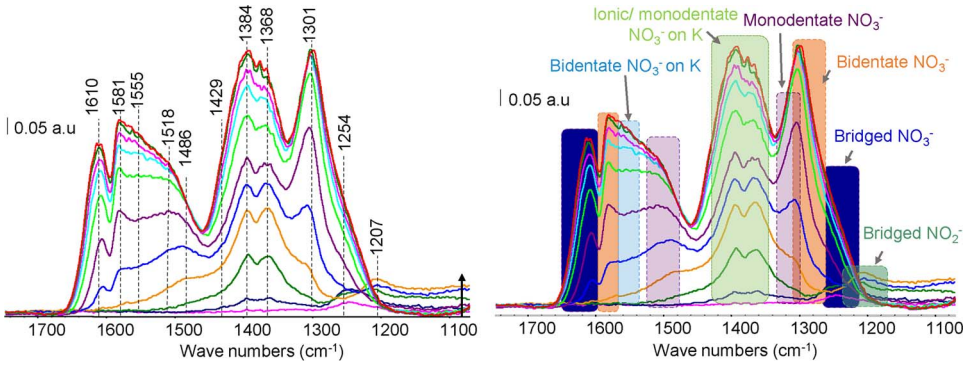

Fig. 3. IR spectra evolution obtained during 'regular' NO_2 adsorption over Pt/ZT + K catalyst with identification of peaks (left) and assignment of NO_x surface species (right). *Note*: different vibration modes of a species are indicated by bars with the same color. (For interpretation of the references to color in this figure legend, the reader is referred to the web version of the article.)

experiments to minimize effect of the NO oxidizing step on the formation of NO_x surface species.

Fig. 3(left) shows evolution of IR spectra during introduction of doses of NO_2 over Pt/ZT + K sample. At very first NO_2 doses, a band at 1207 cm^{-1} assigned for nitrite species can be observed. This band increased up to about 1 mmol/g but then quickly diminished. One of the bands typical for bridged nitrate species at about 1254 cm^{-1} also increases at early stage, however, its intensity then seems to suspend. The other high wavenumber associated band for this bridged NO_3^- species at about 1610 cm^{-1} starts increasing a bit later, but keeps growing when more NO_2 doses is introduced. As a consequence, it is suggested that the 1254 cm^{-1} peak may fortuitously characterize both a second type of NO_2^- species at early stage and bridged NO_3^- at higher coverage level. Monodentate/ionic NO_3^- species over K sites, represented by a pair of bands at about 1368 and 1384 cm^{-1} then appear very quickly. Their intensity reaches a high value, convincing that a large amount of potassium monodentate/ionic nitrates is favored on the ZT supported catalyst, as was also reported for alumina based formulation [18]. The evolutions of surface species on both catalytic formulations are similar to those obtained in the case of barium loaded catalysts reported in [27], ionic nitrate species over NO_x storage material being obviously observed. Fig. 3(right) shows all assigned bands for different adsorbed NO_x where species surely arising from interaction with K sites are specified. When not indicated, the nitrates bands correspond to species interacting with the ZT support.

The comparison between 'regular' NO_x adsorption over the two NSMs, K vs. Ba, is shown in Fig. 4. Ionic/monodentate nitrates on the Ba catalyst are obviously more abundant than on the K sample. This can be explained by the fact that the nominal loading of Ba is higher than that of K (0.24 and 0.15 atom nm^{-2} respectively). In addition, one Ba atom can theoretically store two nitrate species ($Ba(NO_3)_2$), which represents twice what one K atom can do (KNO_3). In a consistent manner, nitrate species over the ZT support (< 1300 cm^{-1} or > 1500 cm^{-1}) remain higher on the K loaded sample than that on the Ba sample.

Stability of the adsorbed species on K loaded catalyst was then

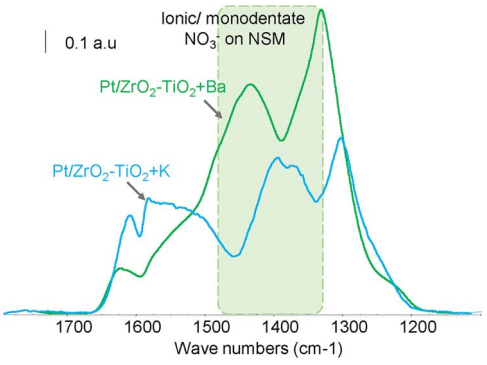

Fig. 4. Comparison of IR spectra obtained for Pt/ZT + K and Pt/ZT + Ba during 'regular' NO_2 adsorption at coverage level of 1.69 mmol/g cat NO_2.

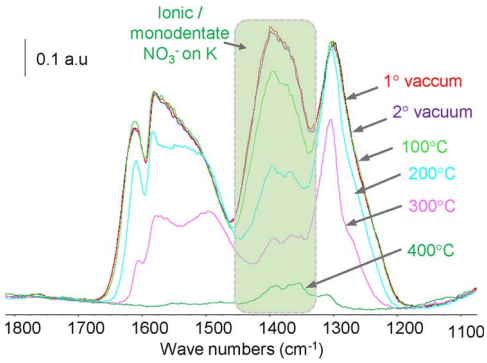

Fig. 5. Evolution of IR spectra obtained during TPD experiment for Pt/ZT + K catalyst.

examined in subsequent TPD experiments, whose results are represented in Fig. 5. As temperature increases, the peak at around 1400 cm^{-1}, standing for monodentate and/or ionic nitrates, diminishes more quickly than other bands (bridged/bidentate). When temperature increases above 300 °C, this band however is more stable than the other bands and even remains at 400 °C. This result suggests that the peak is contributed by both monodentate and ionic species. The species that remains stable at 400 °C is likely ionic nitrate over K sites (KNO_3). Similar behaviour was actually observed for Pt / ZT + Ba in our previous work (see supporting information in Ref. [27]). This observation reaffirms our hypothesis regarding the effect of support material, proposing that ZT support promotes formation of more and finer particles of barium nitrates compared to alumina support [27].

In the second series of experiments for NO_2 adsorption, so called heat-assisted adsorption (Ex2 in Fig. 1), after introduction of NO_2 aliquots the sample was lifted up to the oven set at 380 °C for a duration of 5 min, during which NO_x adsorption/diffusion took place. The sample was then brought down back to the position for IR recording with some delay to ensure the sample is cooled down to room temperature. It is widely known that heat disfavours the formation of unstable nitrite species and thus it was expected that those bands for nitrite species at 1207 cm^{-1} were insignificant on IR spectra (Fig. 6). Other surface species such as ionic, bidentate, monodentate nitrates can be detected and presented in right part of Fig. 6.

For clarification of the effect of heat treatment on NO_x adsorption, IR spectra obtained in Ex1 or Ex2 at similar NO_x uptake for Pt/ZT + K and Pt/ZT + Ba catalysts are presented on the same coordinate, as represented in Fig. 7. On K loaded catalyst (left part), ionic/monodentate nitrate species over K sites (band 1310–1420 cm^{-1}) actually present a decay of their intensity upon heating. On the contrary, bidentate nitrate species on the K phase (bands at about 1300 cm^{-1} and 1500 cm^{-1}) possess an increased intensity. It can also be observed that the bidentate species over TiO_2 (bands at 1530–1590 cm^{-1}) also decrease in the heat-assisted experiment. As seen in Fig. 7, these phenomena on the Pt/ZT + K formulation are highly different from those for Pt/ZT + Ba, on which the ionic nitrate species are promoted upon

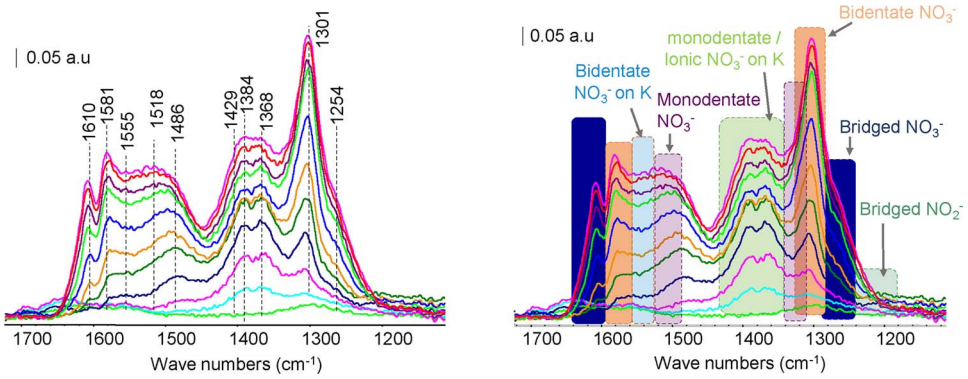

Fig. 6. IR spectra evolution obtained during 'heat-assisted' NO_2 adsorption over Pt/ZT + K catalyst with identification of peaks (left) and assignment of NO_x surface species (right). *Note*: different vibration modes of a species are indicated by bars with the same color. (For interpretation of the references to color in this figure legend, the reader is referred to the web version of the article.)

heating while other species such as bidentate and bridged nitrates are disfavoured.

The distinct behaviour of NO_x adsorption on Pt/ZT + K sample compared to other samples is interesting and suggests an in depth investigation of the NO_x formation mechanism on this NSR formulation. The lower nominal loading of K compared to Ba leads to higher availability of the support for NO_x adsorption, or in another word, amount of nitrate/nitrite on support (Zr or Ti) is higher. Such species are more mobile and would easily transform to nitrate/nitrite over the K phase. This would explain the decrease of bidentate NO_3^- on TiO_2 (wavenumber of about 1530–1590 cm^{-1}). Due to the low loading of K, KNO_3 formed at room temperature likely exists mostly in form of monodentate rather than ionic species ($\nu_a(NO_2)$ expected in the same range) that are the most stable ones. Therefore, when heat is provided, transformation of the less stable K monodentate species into a more stable one is favored most probably through re-dispersion of K onto the ZT support (which is also consistent with the decrease of bidentate NO_3 on TiO_2). The K loading being too low to allow a full coverage of the ZT support upon K migration, the K/support interaction remains important preventing the formation of purely ionic KNO_3. As a consequence, the most stable potassium nitrates that may form in these conditions would consist in bidentate NO_3^-. This is actually the observation through the increase of IR bands typical for K bidentate NO_3^- at around 1300 cm^{-1} and 1500 cm^{-1} in Fig. 7(left).

3.2. NO_x adsorption under operando conditions

As a complementary approach, *operando* experiments were carried out to study NO_x storage phenomena under dynamic conditions at two extreme temperatures, 200 and 450 °C. In these experiments, the NO_x adsorption was studied either feeding NO_2 or NO as NO_x precursors. In the first series of experiments, 400 ppm NO_2 (high purity bottle from Air Liquide), in mixture with 1% O_2 balanced by Ar) was used to minimize the effect of the NO to NO_2 oxidation that has been reported as the rate determining step during NSR operation [29–31]. In the second series of experiments, 300 ppm NO (high purity bottle from Air Liquide), in mixture with 1% O_2 balanced by Ar) was used as feeding gas and thus the nitration process was studied including the NO-to-NO_2 oxidation step. The flow rate was set to fix a GHSV of 100,000 h^{-1}.

Fig. 8 (higher part) shows evolutions of the first 250 sec IR spectra obtained for potassium and barium loaded ZT catalysts under NO_2 nitration condition at 200 °C. Based on the in situ results in Section 3.1, one can recognize the presence of various NO_x adsorbed species such as bridged nitrite, bidentate nitrate, ionic nitrate on both catalytic formulations. It is interesting and obvious that proportions of those species and their variations are distinct between K- and Ba-loaded catalysts. On K-loaded NSR catalyst (Fig. 8, left part), nitrites species (at around 1220 cm^{-1}) and monodentate/ionic nitrate species over K sites (KNO_3, at around 1400 cm^{-1}) start growing simultaneously as better indicated by the green colour contour (Fig. 8, left lower part for which the color reflects the peaks intensity increasing in order: blue, green, yellow, red and for which the full time range equals 500 s). In contrast, the nitrite species on Ba-loaded sample solely and strongly grows right at the beginning of the experiment ($t = 0$) as depicted on the bottom-right part of Fig. 8 (full time range = 500 s). Bridged NO_2^- (1220 cm^{-1}) are thus formed exclusively upon interaction of NO_2 with the Ba catalyst during the first instant of reaction during which nitrates formation can be ruled out. Significant amount of monodentate/ionic NO_3^- (1420–1330 cm^{-1}) only start to be detected after a 100 s delay. The nitrite species on Ba sample continues rising up to about 220 s from which they start to decrease but always remaining co-existing with nitrate species on the surface during the experiments. It should be noted that with the K-loaded sample the detected nitrite species disappeared shortly after the monodentate/ionic nitrate species became dominant. In order to summarize, it is worth emphasizing on the fact that when dealing with NO_2 trapping at 200 °C, K based formulation never leads to formation of NO_2^- alone (without concomitant presence of NO_3^-) while Ba based formulation never leads to formation of NO_3^- alone (without concomitant presence of NO_2^-). These differences may be explained by a much higher nitrite stability over the Ba-loaded catalyst and by distinct routes for NO_x adsorption as discussed below.

The evolution of surface species may also provide explanations for the differences in the gas phase profiles at outlet for each catalyst (Fig. 9). For K-loaded sample, NO_2 adsorption is faster than that on Ba-

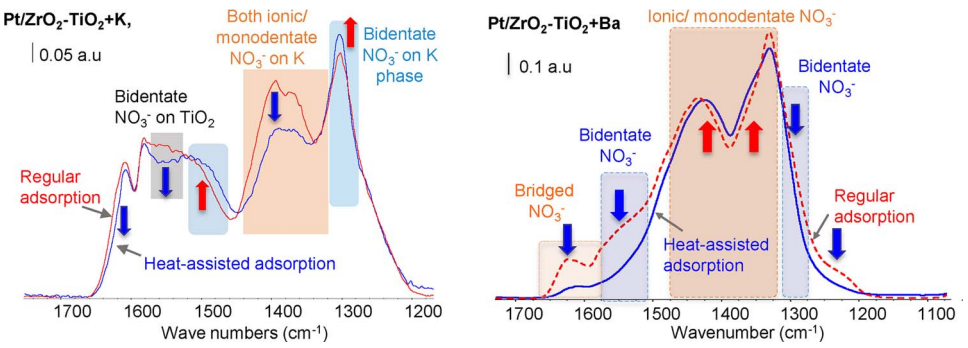

Fig. 7. Comparison between IR spectra obtained during 'regular' and 'heat-assisted' NO_2 adsorption over Pt/ZT + K (left) and Pt/ZT + Ba (right) catalysts. *Note*: red and blue arrows are added for indication of respective increasing and decreasing trends of the peaks. (For interpretation of the references to color in this figure legend, the reader is referred to the web version of the article.)

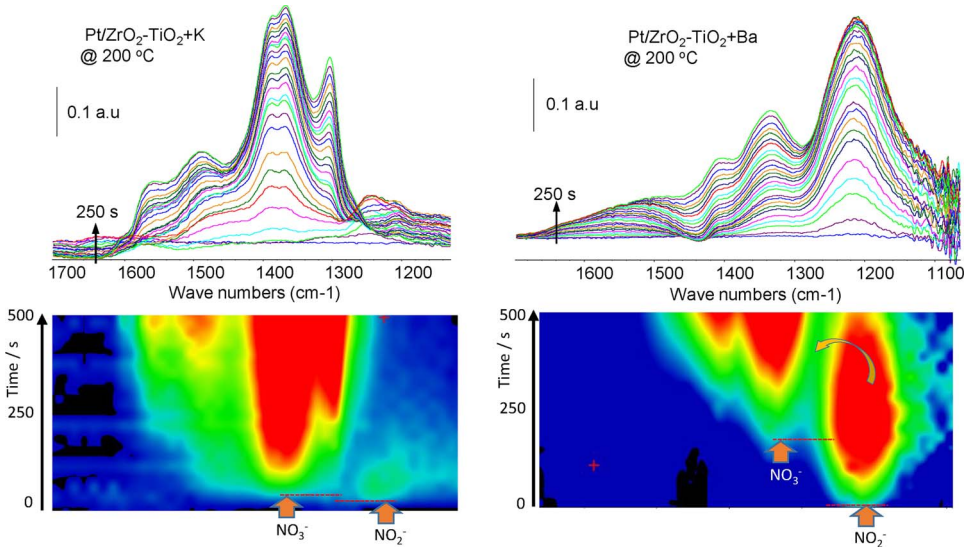

Fig. 8. IR spectra showing evolution of surface species during first 250 s (upper part) and 500 s (lower part) NO_2 nitration over Pt/ZT + K (left) and Pt/ZT + Ba (right) at 200 °C (time resolution 10 s, the color in lower part reflects the peaks intensity of IR spectra increasing in order: blue, green, yellow, red). (For interpretation of the references to color in this figure legend, the reader is referred to the web version of the article.)

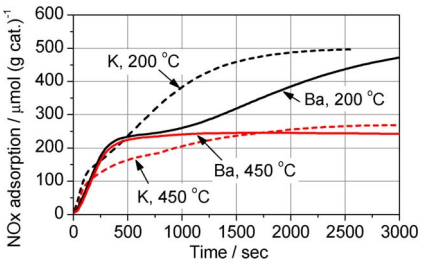

Fig. 9. Gas phase analysis during NO_2 nitration over Pt/ZT + K and Pt/ZT + Ba catalysts at 200 or 400 °C.

loaded one at the beginning but then slightly slows down with a small wave on the profile. Timing of this wave is in good agreement with the end of simultaneous nitrite/nitrate formation and start of the single monodentate/ionic nitrate rise, which would proceed at a lower rate. For the Ba-loaded sample, the profile shows an obvious 'transition plateau' regime up to about 1000 s. This plateau was related to the slow conversion of nitrite into nitrate species [27] without (or little) additional adsorption of NO_x from gas phase. This agrees with the fact that nitrite species accumulate as the most dominant adsorbed species during the first moment of the adsorption process (Fig. 8, right part) and further require their oxidation into superficial NO_3^- (transition plateau) before diffusion into the bulk of Ba particles (characterized by the new NO_x uptake at the end of the plateau).

Taking now into account both the adsorbed surface species and the simultaneous gas phase evolution at 200 °C one may suggest an explanation for the catalytic distinct behaviours. For the potassium based formulation, when NO_2 is fed the adsorption mostly initiates through the disproportionation mechanism leading to the simultaneous formation of NO_3^- and NO_2^-. It has indeed been previously reported that NO_3^- formation is detected from NO_2 disproportionation over a basic Na-MOR sample at temperatures as low as 25 °C [32]. Furthermore, it was later evidenced over a series of alkaline (Li, Na, K, Rb) basic zeolites that NO_2 disproportionation not only always proceeds at room temperature but also that the alkaline cation chemical hardness plays a key role in the nitrate formation [33]. Indeed, isolated hard cations generate a rather high surrounding electrostatic field that favours polarization of chemical bonds. In the case of NO_2 disproportionation, the intermediate dimeric N_2O_4 species would thus more efficiently split into NO^+ and NO_3^- in presence of a rather hard cation, such as dispersed K^+ in the present work. In summary, the initial global reaction would be:

$$K^+ - O^{2-} - K^+ + 2\ NO_2 \rightarrow K^+ — O^{2-} — NO^+ + K^+NO_3^- \rightarrow KNO_2^- + KNO_3^-$$

Then, once the surface reaches a given coverage level, NO_2^- are subsequently oxidized into most stable NO_3^- and nitrites completely disappear from the catalyst surface.

On the contrary, for the barium based formulation, when NO_2 is fed at 200 °C the adsorption process initiates only via the primary formation of single NO_2^- species. The Ba cations chemical hardness would thus be too low to enable the disproportionation mechanism and stable NO_2^- then accumulate on the surface through a kind of 'nitrite' route that was reported to be platinum assisted [34]. The present results however suggest a slightly distinct mechanism that that initially described for the so-called nitrite route for which NO_2^- only appears when NO + O_2 was fed in the [150–250 °C] temperature range [34]. Indeed, in a complementary study where NO_2 was fed with or without O_2 over both Ba/Al_2O_3 and $Pt\text{-}Ba/Al_2O_3$ catalysts, an extensive storage in the form of ionic nitrates occurred at all the temperatures studied, without formation of any nitrites [35]. In order to make the whole results consistent, a strong support effect is suggested in which specific interaction between Ba and ZT would be involved. Indeed, it should be emphasized that our present formulation is based on a Ti containing support (30wt% TiO_2) whose electron transfer ability may favour the nitrite formation from fed NO_2 while the alumina properties would not allow such a possibility.

Regarding the effect of temperature on the NO_x adsorption, when dealing with the K loaded sample, a similar behaviour was observed for the NO_x adsorption and gas phase profiles at 450 °C (Fig. 9, red curves), indicating a similar pathway: disproportionation followed by NO_2^- oxidation. On the contrary, the Ba loaded sample does not present anymore the 'transition plateau' since at 450 °C the NO_2^--to-NO_3^- oxidation or migration of NO_3^- towards the bulk no longer represent determining steps.

In order to examine NO_x adsorption taking into account NO-to-NO_2 oxidation step, similar experiments were performed using NO as the feed gas. Fig. 10 shows evolutions of IR spectra obtained for the two catalyst formulations at 200 and 450 °C. It can be recognized that both samples adsorb a lot of NO_x in the form of nitrite species (wavenumber at about 1230 cm^{-1}) at the lower temperature of 200 °C, while more nitrate species were observed at the high temperature.

Fig. 11 represents the NO_x adsorption analysis for nitration experiments using NO, showing that the K-loaded catalyst possesses a slightly higher adsorption rate compared to the Ba-loaded sample at the very early stage (less than 250 s) at either high or low temperature. Both samples seem to reach their saturation after about 300 s. It thus clearly appears from the above results obtained with fed NO instead of

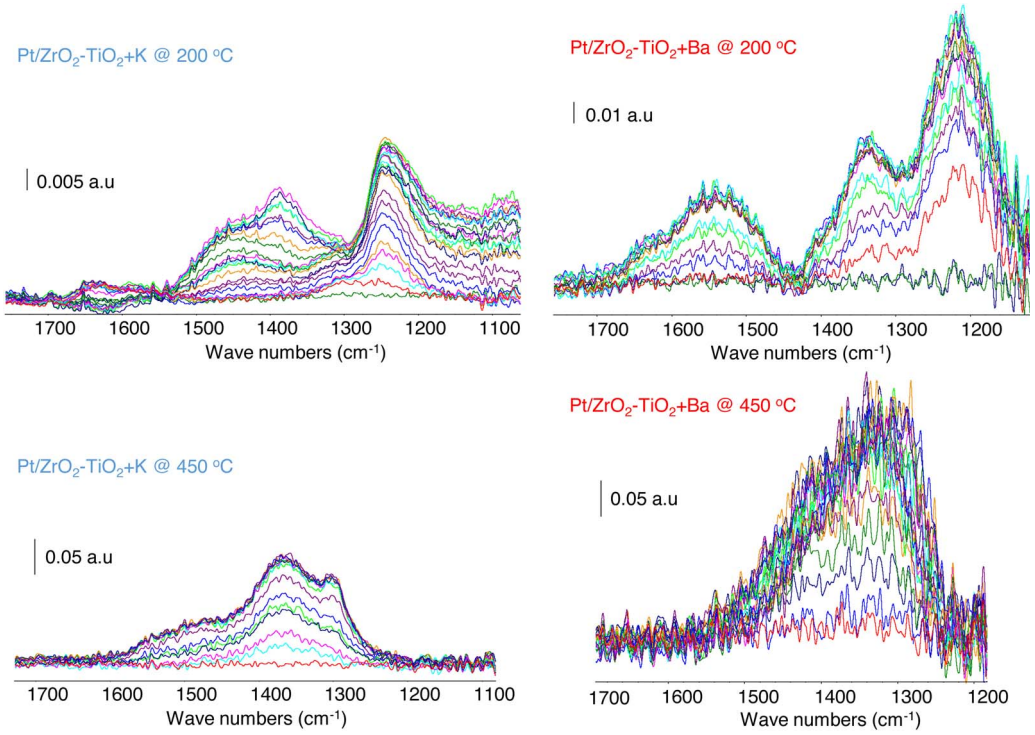

Fig. 10. IR spectra showing surface evolution during NO nitration over Pt/ZT + K (left) and Pt/ZT + Ba (right), at 200 °C (top) and 450 °C (bottom). (time resolution 10 s).

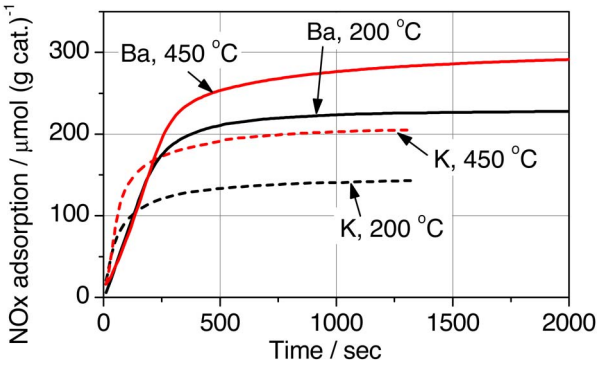

Fig. 11. Gas phase analysis during NO nitration over Pt/ZT + K (dash line) and Pt/ZT + Ba (solid line) catalysts at 200 or 450 °C.

fed NO_2 that given the rather low NO to NO_2 oxidation efficiency expected at 200 °C the NO_2 concentration in the reactant flow is too low to substantially feed the disproportionation path. As a consequence, the 'nitrite' route is now the main path for NO_x adsorption through mostly NO_2^- accumulation for both catalytic formulations. The faster trapping for the K based catalyst could be related to the higher availability of K^+ cations being obviously more dispersed than Ba^{2+} ones over the ZT support (lower nominal amount of potassium and different behaviour upon heating: see Section 3.1).

Table 1 summarizes the total NO_x adsorption when feeding with NO_2 or NO at different temperatures. The adsorbed amount of NO_2 over K at low *T* is higher than that over Ba catalyst, while at high temperatures 450 °C the amounts are similar for both catalysts. On the contrary, the adsorbed amount of NO is always higher on the Ba loaded catalyst whatever the adsorption temperature.

As discussed in the previous section, at 200 °C K^+ sites favour the NO_2 disproportionation mechanism for NO_x adsorption, leading to early formation of NO_3^- that accumulate faster and to a higher extent onto the support. On the contrary, for the Ba-loaded sample, the consecutive formation of nitrates according to $NO_2^- \rightarrow NO_3^- \rightarrow$ bulk $BaNO_3^-$ proceeds more slowly with (almost) no involvement of the ZT support. This would explain why at 200 °C, the K-loaded sample adsorb more NO_2 than the Ba-loaded one. At higher temperature, *i.e.* 450 °C, the formation of NO_3^- and its diffusion into the bulk are no longer the rate determining steps, and as the higher density of Ba sites compared to that of K sites leads to the higher total NO_x adsorption on Ba-loaded catalyst.

Table 1
Total NO_x trapped on catalysts at different temperatures (µmol/g cat).

Feeding gas	*T* (°C)	NO_x trapped (µmol/g cat)	
		Pt/ZT + K	Pt/ZT + Ba
NO_2	200	512	422
	450	260	254
NO	200	143	224
	450	205	297

3.3. Surface/gas phase interaction under isotopic labelling study

It is important to understand the exchange between gaseous NO_x and adsorbed NO_x species as this will provide more insight into to the catalytic mechanisms for NO_x trapping over the catalysts. Isotopic labelling using different isotopes of nitrogen, ^{14}N and ^{15}N, is useful to distinguish different 'kinds' of nitrogen-containing species. Such methodology has already been used to study NSR catalyst elsewhere [36]. According to these authors, the exchange of ^{15}N and ^{14}N species follows the steps as below:

$$^{15}NO + {}^{14}NO_3^- \rightleftharpoons [O = {}^{15}N - O - {}^{14}N = (O)_2]^- \quad (1)$$

$$\rightleftharpoons [(O)_2 - {}^{14}N - O - {}^{15}N - O]^- \quad (2)$$

$$\rightleftharpoons {}^{14}NO + {}^{15}NO_3^- \quad (3)$$

The authors also suggested a similar mechanism for $^{14}N - {}^{15}N$ exchange between $^{14}NO_2^-$ and ^{15}NO via intermediate dimers [O = ^{15}N-O-

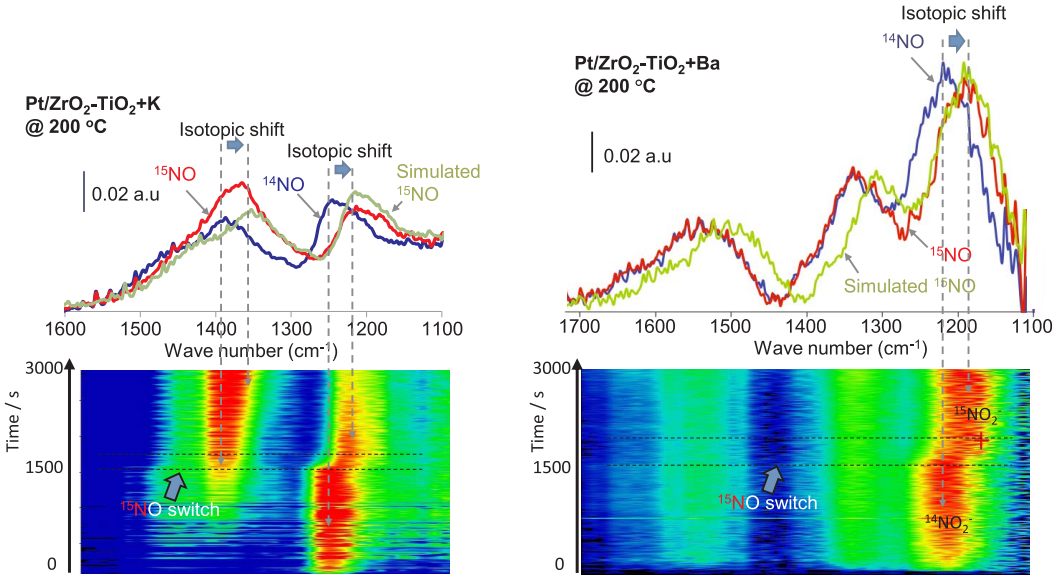

Fig. 12. Lower parts: 2D-evolution of IR spectra obtained during isotopic labelling experiments at 200 °C for Pt/ZT + K (left) and Pt/ZT + Ba (right) (the horizontal dash lines are added for indication of 'exchanging period'). Upper parts: IR spectra recorded at the end of ^{14}NO and ^{15}NO feeding, in comparison to the simulated spectra representing 100% ^{15}N exchange.

$^{14}N=O]^-$ or $[O=^{15}N\text{-}O\text{-}^{14}N=(O)2]^-$, resulting in $^{15}NO_2^-$ and ^{14}NO. This implies that any NO_x species are necessarily exchanged through NO-Ba (or NO-K) bond breaking. Therefore, the exchange between species on the catalyst surface and in gas phase will be here monitored in order to learn more about the distinct NO_x storage paths.

In the present work, new nitration experiments were carried out at the two previously chosen temperatures (200 and 450 °C) but feeding in a first step with a flow made of ^{14}NO for 1500 s followed by a second step with ^{15}NO feed gas (15N 98% from CK ISOTOPES) in another 1500 s period. During the whole experiment period, surface species and gas phase were simultaneously monitored by both IR and chemiluminescence analytics. Figs. 12 and 13 show the surface evolution and gas phase analysis respectively for the two catalysts Pt/ZT + K and Pt/ZT + Ba at 200 °C. The lower subfigures in Fig. 12 represent the evolution of the IR band intensity for surface species during gas feeding (same color code as that used in Fig. 8). The dash-line indicates the moment for switching from ^{14}NO to ^{15}NO. After the isotopic switch, IR peaks corresponding to nitrite $^{14}NO_2^-$ (at around 1200 cm^{-1}) start shifting on both samples towards lower wavenumber, indicating the conversion into $^{15}NO_2^-$. These shifts are in good agreement with the isotopic effect prediction described in [36]. Based on the quantitative estimation suggested in that work, we have simulated theoretical spectra for 100% exchange as depicted in the upper parts of Fig. 12 (green spectra). The comparison between the simulated and the experimental spectra obtained at the end of the ^{15}NO period (red spectra) indeed shows a perfect wavenumber match. It can however be observed a distinct 'exchange' behaviour depending on the catalyst composition as being discussed below.

For the K-loaded catalyst the whole IR peaks shifted towards lower wavenumber and the main envelope for the experimental ^{15}NO spectrum and the theoretical one superimpose, that reveals the presence of similar species. However, the band intensities do not match: the theoretical spectrum 'predicts' a higher amount of $^{15}NO_2^-$ and a lower amount of NO_3^- (mix of ^{14}N and ^{15}N ones at 1400 and 1360 cm^{-1} respectively) than experimentally observed. This is an important information since it reveals the un-equilibrated state of the sample after the preliminary ^{14}NO feeding period. In fact, it provides clear evidence that not only NO_2^- exchange proceeds but also, although rather slow, their conversion into nitrates operates at 200 °C.

For the Ba-loaded sample, the isotopic shift can be observed only for nitrite species (at about 1200 cm^{-1}) while the other peaks at about 1350 and 1550 cm^{-1} remains unchanged. Based on their wavenumbers, these two later peaks might correspond to monodentate/ionic and bidentate $^{14}NO_3^-$ nitrates, respectively [27]. It is worth noting that the NO_2^- exchange is complete as evidenced by the perfect match of the bands corresponding to the ^{15}NO experimental and the ^{15}NO theoretical spectra. On another hand, the two bands typical for nitrates (peaks at about 1350 and 1550 cm^{-1}) remain un-exchanged, thus revealing their strong interaction with the involved NO_x storage material. Only part of all the adsorbed NO_x species is thus able to exchange from ^{14}NOx to ^{15}NOx. A complementary quantification from the gas phase analysis allowed to estimate the total amount of ^{14}NOx trapped from 0 to 5 min period in Fig. 13 while the total amount of exchanged $^{15}NO_x$ was determined from 25 to 30 min period in Fig. 13. Both value are

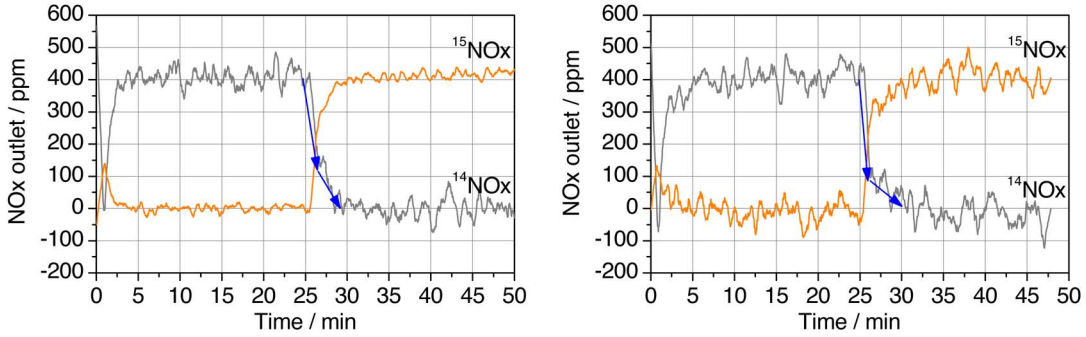

Fig. 13. Concentrations of ^{14}NO and ^{15}NO during *operando* experiments for Pt/ZT + K (left) and Pt/ZT + Ba (right) catalysts at 200 °C. The arrows are added for clarity of different stages in gas concentration profiles.

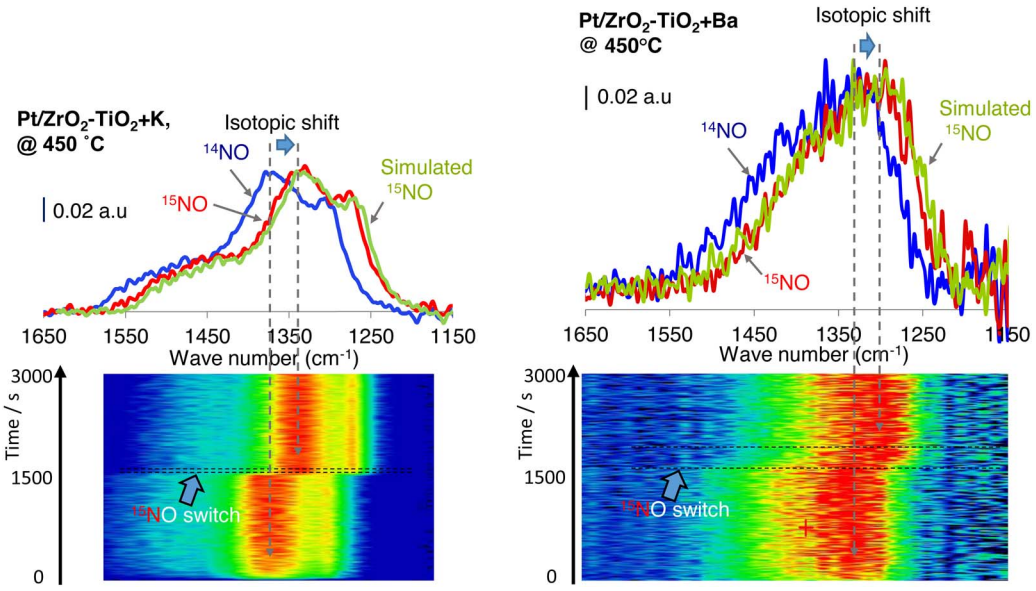

Fig. 14. Lower parts: 2D-evolution of IR spectra obtained during isotopic labelling experiments at 450 °C for Pt / ZT + K (left) and Pt / ZT + Ba (right) (the horizontal dash lines are added for indication of 'exchanging period'). Upper parts: IR spectra recorded at the end of ^{14}NO and ^{15}NO feeding, in comparison to the simulated spectra representing 100% ^{15}N exchange.

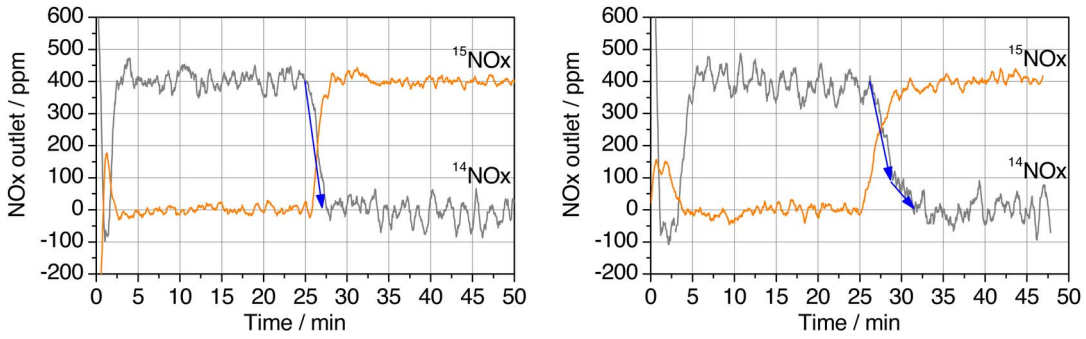

Fig. 15. Concentrations of ^{14}NO and ^{15}NO during isotopic labelling experiments for Pt/ZT + K (left) and Pt/ZT + Ba (right) catalysts at 450 °C. The arrows are added for clarity of different stages in gas concentration profiles.

quite similar (about 230 µmol/g cat. This *a priori* surprising result is nevertheless consistent with the existence of a minority amount of Ba NO_3^- species that would be too stable to allow isotopic exchange at 200 °C. This minority amount of $Ba(NO_3)^-$ upon nitration at 200 °C over Pt/ZT + Ba was previously reported despite relatively intense IR bands due to high molar extinction coefficient for NO_3^- compared to NO_2^- species [27].

A more precise gas phase analysis during the isotopic switch reveals the drop of ^{14}NO simultaneously with the jump of ^{15}NO for both catalysts as seen in Fig. 13. The total exchange time defined as the delay required to drop from stabilized ^{14}NOx outlet to zero upon isotopic switch can be roughly estimated as 180 s and 300 s for K- and Ba-loaded catalysts, respectively. The shorter period for the K based formulation would be simply du to a lower amount of exchanged KNO_2 compared to $Ba(NO_2)_2$. It is noteworthy that the drop of ^{14}NOx (as well as the growth of ^{15}NOx) starts with sharp change and then slows down especially for the Ba catalyst, which may correspond to the exchange of surface species with different stability, for example weaker nitrites at beginning and more stable (sub-superficial) ones later.

At higher temperature 450 °C, the kinetics for all processes including isotopic exchange are known to be faster, it is therefore expected that exchanges between ^{14}N- and ^{15}N-containing species take place completely. This is obviously the case as depicted in Fig. 14 where the $^{14}NO_3^-$, (either over potassium or barium) are 100% converted into $^{15}NO_3^-$. The gas phase analysis (Fig. 15) further indicates a slightly different exchange rate for the two catalysts. A fast and monotonous decay of the ^{14}NO concentration upon isotopic switch for the potassium formulation contrasts with a slower and slope brake comporting decay for the Ba based one. The longer exchange time and two steps evolution for Ba-loaded sample can be again explained by a higher amount of large barium nitrate particles compared to mostly isolated superficial K sites.

4. Conclusions

The present work reports for the first time a detailed study of NO_x uptake over a K-loaded on ZrO_2-TiO_2 NSR catalyst. The *in situ* experiments revealed that NO_x adsorption under heated environment favors bidentate nitrate species (over K sites) rather than ionic nitrate species observed for Ba-loaded NSR catalyst in our previous work [27]. The *operando* experiments with NO and NO_2 revealed different mechanisms of NO_x adsorption over the two NSMs: initial simultaneous NO_2^- and NO_3^- formation over K loaded catalyst while over Ba-loaded one, NO_2^- is strongly accumulated first then converted to NO_3^-. The combination of isotopic labelling and *operando* experiments enabled us to identify distinct dynamic behaviours of the exchange between nitrogen containing adsorbed surface species and gaseous ones. The significance of this work lies on the insights into NO_x adsorption for K loaded NSR catalyst as well as the comprehensive comparison between the two common NO_x storage materials, K and Ba. The work would be

highly beneficial for advanced designing work for complex catalyst converters such as zone-coated technology [37–39], where deeper knowledge on each catalyst component would provide more precise estimation of overall performance for the final catalytic converter.

Acknowledgements

The authors would like to thank colleagues (H. Hirata, M. Sakano, S. Shirakawa, and M. Ibe) in Advanced Material Engineering Div., Toyota Motor Corporation for their discussions and comments on the work.

References

[1] N. Miyoshi, S. Matsumoto, K. Katoh, T. Tanaka, J. Harada, N. Takahashi, K. Yokota, M. Sugiura, K. Kasahara, Development of New Concept Three-Way Catalyst for Automotive Lean-Burn Engines, SAE Technical 950809, (1995).
[2] S. Matsumoto, DeNOx catalyst for automotive lean-burn engine, Catal. Today 29 (1996) 43–45 Second Japan-E, Joint Workshop on the Frontiers of Catalytic Science and Technology for Energy, Environment and Risk Prevention.
[3] A. William, S. Epling, L. Campbell, N. Currier, J. Parks, Overview of the fundamental reactions and degradation mechanisms of NO_x storage/reduction catalysts, Catal. Rev. Eng. 46 (2004) 1–72.
[4] T. Kobayashi, T. Yamada, K. Kayano, Study of NO_x Trap Reaction by Thermodynamic Calculation, SAE Technical 970745, (1997).
[5] I. Nova, L. Lietti, L. Castoldi, E. Tronconi, P. Forzatti, New insights in the NO_x reduction mechanism with H_2 over PtBa/$\gamma-Al_2O_3$ lean NO_x trap catalysts under near-isothermal conditions, J. Catal. 239 (2006) 244–254.
[6] D. James, E. Fourre, M. Ishii, M. Bowker, Catalytic decomposition/regeneration of Pt/Ba$(NO_3)_2$ catalysts: NO_x storage and reduction, Appl. Catal. B 45 (2003) 147–159 Cited By 126..
[7] L. Castoldi, I. Nova, L. Lietti, P. Forzatti, Study of the effect of Ba loading for catalytic activity of PtBa/Al_2O_3 model catalysts, Catal. Today 96 (2004) 43–52 NO_x Abatement in Lean-Burn and Diesel Vehicles..
[8] H. Imagawa, N. Takahashi, T. Tanaka, S. Matsunaga, H. Shinjoh, Improved NO_x storage-reduction catalysts using Al_2O_3 and ZrO_2-TiO_2 nanocomposite support for thermal stability and sulfur durability, Appl. Catal. B 92 (2009) 23–29 Cited By 15..
[9] G. Liu, P.-X. Gao, A review of NO_x storage/reduction catalysts: mechanism, materials and degradation studies, Catal. Sci. Technol. 1 (2011) 552–568.
[10] S. Matsumoto, Y. Ikeda, H. Suzuki, M. Ogai, N. Miyoshi, NO_x storage-reduction catalyst for automotive exhaust with improved tolerance against sulfur poisoning, Appl. Catal. B 25 (2000) 115–124.
[11] M. Hirano, C. Nakahara, K. Ota, O. Tanaike, M. Inagaki, Photoactivity and phase stability of ZrO_2-doped anatase-type TiO_2 directly formed as nanometer-sized particles by hydrolysis under hydrothermal conditions, J. Solid State Chem. 170 (2003) 39–47.
[12] H. Chen, J. Shi, W. Zhang, M. Ruan, D. Yan, Incorporation of titanium into the inorganic wall of ordered porous zirconium oxide via direct synthesis, Chem. Mater. 13 (2001) 1035–1040.
[13] N. Nejar, M. Illan-Gomez, Potassium copper and potassium cobalt catalysts supported on alumina for simultaneous NO_x and soot removal from simulated diesel engine exhaust, Appl. Catal. B 70 (2007) 261–268 Papers presented at the 4th International Conference on Environmental Catalysis (4th ICEC) Heidelberg, Germany, June 05 '08, 2005..
[14] M. Cortes-Reyes, M. Herrera, I. Pieta, M. Larrubia, L. Alemany, In-situ TG-MS study of NO_x and soot removal over LNT model catalysts, Appl. Catal. A 523 (2016) 193–199.
[15] T. Toops, N. Ottinger, C. Liang, J. Pihl, E. Payzant, Impact of dopants on the sulfation, desulfation and NO_x reduction performance of Ba-based NO_x storage-reduction catalysts, Catal. Today 160 (2011) 131–136.
[16] J.-S. Choi, W.P. Partridge, C.S. Daw, Spatially resolved in situ measurements of transient species breakthrough during cyclic, low-temperature regeneration of a monolithic Pt/K/Al_2O_3 NO_x storage-reduction catalyst, Appl. Catal. A 293 (2005) 24–40.
[17] T.J. Toops, D.B. Smith, W.P. Partridge, Quantification of the in situ DRIFT spectra of Pt/K/γ-Al_2O_3 NO_x adsorber catalysts, Appl. Catal. B 58 (2005) 245–254.
[18] L. Castoldi, L. Lietti, I. Nova, R. Matarrese, P. Forzatti, F. Vindigni, S. Morandi, F. Prinetto, G. Ghiotti, Alkaline- and alkaline-earth oxides based Lean NO_x traps: effect of the storage component on the catalytic reactivity, Chem. Eng. J. 161 (2010) 416–423 Catalysis by acids and bases: process and engineering aspects.
[19] D.H. Kim, K. Mudiyanselage, J. Szanyi, J.H. Kwak, H. Zhu, C.H. Peden, Effect of K loadings on nitrate formation/decomposition and on NO_x storage performance of K-based NO_x storage-reduction catalysts, Appl. Catal. B 142 (2013) 472–478.
[20] T.J. Toops, D.B. Smith, W.S. Epling, J.E. Parks, W.P. Partridge, Quantified NO_x adsorption on Pt/K/$\gamma-Al_2O_3$ and the effects of CO_2 and H_2O, Appl. Catal. B 58 (2005) 255–264.
[21] T.J. Toops, D.B. Smith, W.P. Partridge, NO_x adsorption on Pt/K/Al_2O_3, Catal. Today 114 (2006) 112–124 Catalytic control of diesel exhaust emissions.
[22] I. Malpartida, M. Guerrero-Perez, M. Herrera, M. Larrubia, L. Alemany, MS-FTIR reduction stage study of NSR catalysts, Catal. Today 126 (2007) 162–168.
[23] Y. Sakamoto, S. Matsunaga, K. Okumura, T. Kayama, K. Yamazaki, N. Takahashi, T. Tanaka, Y. Kizaki, T. Motohiro, H. Shinjoh, Comparison between the NO_x release-reduction reaction for Pt/Ba/Al_2O_3 and Pt/K/Al_2O_3 on a millisecond time scale, Chem. Eng. Sci. 63 (2008) 5028–5034.
[24] D. Kim, K. Mudiyanselage, J. Szanyi, J. Hun Kwak, H. Zhu, C. Peden, Understanding the NO_x storage process in NO_x storage-reduction catalysts: similarities and differences between Ba and K, Anaheim, CA, Conference of 241st ACS National Meeting and Exposition: 27–31 March (2011).
[25] S. Morandi, F. Prinetto, L. Castoldi, L. Lietti, P. Forzatti, G. Ghiotti, Effect of water and ammonia on surface species formed during NO_x storage-reduction cycles over Pt-K/Al_2O_3 and Pt-Ba/Al_2O_3 catalysts, Phys. Chem. Chem. Phys. 15 (2013) 13409–13417.
[26] M. Piacentini, M. Maciejewski, A. Baiker, Supported Pt-Ba NO_x storage-reduction catalysts: influence of support and Ba loading on stability and storage efficiency of Ba-containing species, Appl. Catal. B 66 (2006) 126–136.
[27] S.P.D. Valle, O. Marie, H.P. Nguyen, Effect of support material Al_2O_3 vs ZrO_2-TiO_2 on the Ba availability for NSR catalyst: an in situ and operando IR study, Appl. Catal. B 223 (2018) 116–124.
[28] M. Ahrens, O. Marie, P. Bazin, M. Daturi, Fe-H-BEA and Fe-H-ZSM-5 for NO_2 removal from ambient air – A detailed in situ and operando FTIR study revealing an unexpected positive water-effect, J. Catal. 271 (2010) 1–11.
[29] S.S. Chaugule, A. Yezerets, N.W. Currier, F.H. Ribeiro, W.N. Delgass, Fast NO_x storage on Pt/BaO/$\gamma-Al_2O_3$ lean NO_x traps with NO_2+O_2 and $NO+O_2$: effects of Pt, Ba loading, Catal. Today 151 (2010) 291–303 Diesel emissions control catalysis.
[30] M. AL-Harbi, W.S. Epling, Investigating the effect of NO versus NO_2 on the performance of a model NO_x storage/reduction catalyst, Catal. Lett. 130 (2009) 121–129.
[31] I. Nova, L. Lietti, P. Forzatti, Mechanistic aspects of the reduction of stored NO_x over Pt-Ba/Al_2O_3 lean NO_x trap systems, Catal. Today 136 (2008) 128–135 Catalytic control of emissions from diesel-powered vehicles.
[32] C. Henriques, O. Marie, F. Thibault-Starzyk, J.-C. Lavalley, NO^+ ions as IR probes for the location of OH groups and Na^+ ions in main channels and side pockets of mordenite, Microporous Mesoporous Mater. 50 (2001) 167–171.
[33] O. Marie, N. Malicki, C. Pommier, P. Massiani, A. Vos, R. Schoonheydt, P. Geerlings, C. Henriques, F. Thibault-Starzyk, NO_2 disproportionation for the IR characterisation of basic zeolites, Chem. Commun. (2005) 1049–1051.
[34] L. Lietti, M. Daturi, V. Blasin-Aubé, G. Ghiotti, F. Prinetto, P. Forzatti, Relevance of the nitrite route in the NOx adsorption mechanism over Pt-Ba/Al_2O_3 NO*x* storage reduction catalysts investigated by using Operando FTIR spectroscopy, Chem. Cat. Chem. 4 (2012) 55–58.
[35] F. Prinetto, G. Ghiotti, I. Nova, L. Castoldi, L. Lietti, E. Tronconi, P. Forzatti, In-situ FT-IR and reactivity study of NO storage over Pt-Ba/Al_2O_3 catalysts, Phys. Chem. Chem. Phys. 5 (2003) 4428–4434.
[36] R.V. Mikhaylov, A.A. Lisachenko, B.N. Shelimov, V.B. Kazansky, G. Martra, S. Coluccia, FTIR and TPD study of the room temperature interaction of a NO-oxygen mixture and of NO_2 with titanium dioxide, J. Phys. Chem. C 117 (2013) 10345–10352.
[37] R.M. Heck, R.J. Farrauto, S.T. Gulati (Eds.), Catalytic Air Pollution Control: Commercial Technology, John Wiley & Sons, 2009.
[38] X. Karatzas, J. Dawody, A. Grant, E. Svensson, L. Pettersson, Zone-coated Rh-based monolithic catalyst for autothermal reforming of diesel, Appl. Catal. B 101 (2011) 226–238.
[39] C.-Q. Zhou, G.-J. Dong, F. Gong, X. Chang, Preparation and characterization of monolith catalysts loaded with copper and manganese for low-temperature NH_3-SCR, Ranliao Huaxue Xuebao/J. Fuel Chem. Technol. 37 (2009) 588–594.